Inhibitor selectivity: profiling and prediction

Janssen, A.P.A.

If you don't know where you are going,
any road will take you there.
George Harrison

6 Development of a multiplexed ABPP assay to evaluate activity of endocannabinoid hydrolase inhibitors

This research was published in A.P.A. Janssen, D. van der Vliet *et al.*, *ACS Chem. Biol.* **13**, 2406–2413 (2018).

Introduction

All endocannabinoid hydrolases except *N*-acetylphosphatidylethanolamine phospholipase D (NAPE-PLD) belong to the family of serine hydrolases. This family consists of over 200 proteins that use a nucleophilic serine to hydrolyze ester-, amide-, or thioesterbonds in small molecules and proteins via a covalent acyl-protein intermediate.[1,2] This mode of action is exploited in activity-based protein profiling (ABPP).[3,4] The archetypical activity-based probe (ABP) for serine hydrolases is the fluorophosphonate (FP) probe (FP-TAMRA (**1**), Figure 6.1), which was introduced by Liu *et al.* almost 20 years ago.[5] This probe is widely

used to study serine hydrolases in complex proteomes.[6,7] Although the FP-based probes are known for their broad reactivity, they do not react with all serine hydrolases.[4] Most notably, diacylglycerol lipase α (DAGL-α) is amongst the enzymes which cannot be visualized by FP-based ABPs.[8] To study DAGL-α, MB064 ((**2**), Figure 6.1), a tailored chemical probe with a BODIPY-TMR as fluorophore, was developed.[9] In terms of experimental efficiency with respect to time, cost-of-reagents, and use of valuable biological samples, it would be optimal to combine the commercially available FP-TAMRA (ActivX™) and MB064 in the same experiment. However, MB064 cannot be applied in conjunction with FP-TAMRA (**1**), because the excitation/emission spectra of their fluorophores overlap. Therefore, the aim of the current study was to synthesize, characterize and apply a new FP-based probe (**3**) with a different reporter tag (BODIPY-FL) that is compatible with MB064. Such a multiplexed assay, using different activity-based probes, has been shown to work for other enzyme classes in the past.[10–12] Here, a multiplexed ABPP assay with ABP (**3**) and MB064 was developed and used to study endocannabinoid hydrolase activity and to profile inhibitors on activity and selectivity in mouse brain proteomes.

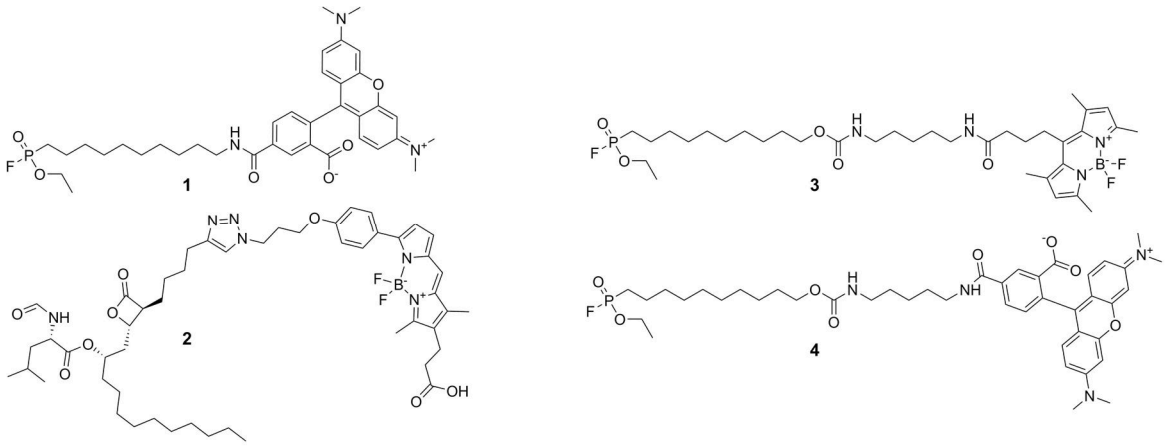

Figure 6.1 | Chemical structures of the four activity-based probes used in this study: FP-TAMRA (**1**), MB064 (**2**), FP-BODIPY (**3**) and a control probe (**4**)

Results and discussion

FP-BODIPY probe (**3**) was synthesized using a previously described method (Scheme S6.1).[13] In addition, commercially available FP-TAMRA (probe **1**) and control compound FP-TAMRA (**4**), containing the same linker as (**3**), were synthesized using similar procedures (Scheme S6.2 and S6.3, respectively).

To obtain a broad view of serine hydrolase labeling by the FP-probes in various tissues, first FP-TAMRA (**1**) and FP-BODIPY (**3**) were incubated with membrane and cytosol fractions of a panel of seven mouse tissues (brain, testes, kidney, spleen, heart, liver and pancreas) at a concentration of 500 nM (Figure 6.2). The proteins were resolved using SDS-PAGE and probe-labeled proteins were visualized by fluorescent scanning of the gel. The overall labeling profile in the various proteomes was comparable between probe **1** and **3**, but several differences were observed, denoted with boxes. In the brain, for example, membrane proteome FP-BODIPY (**3**) labeled additional targets, including in the top left box DAGL-α, the identity of which was confirmed by competition with LEI104 (Figure S6.1).

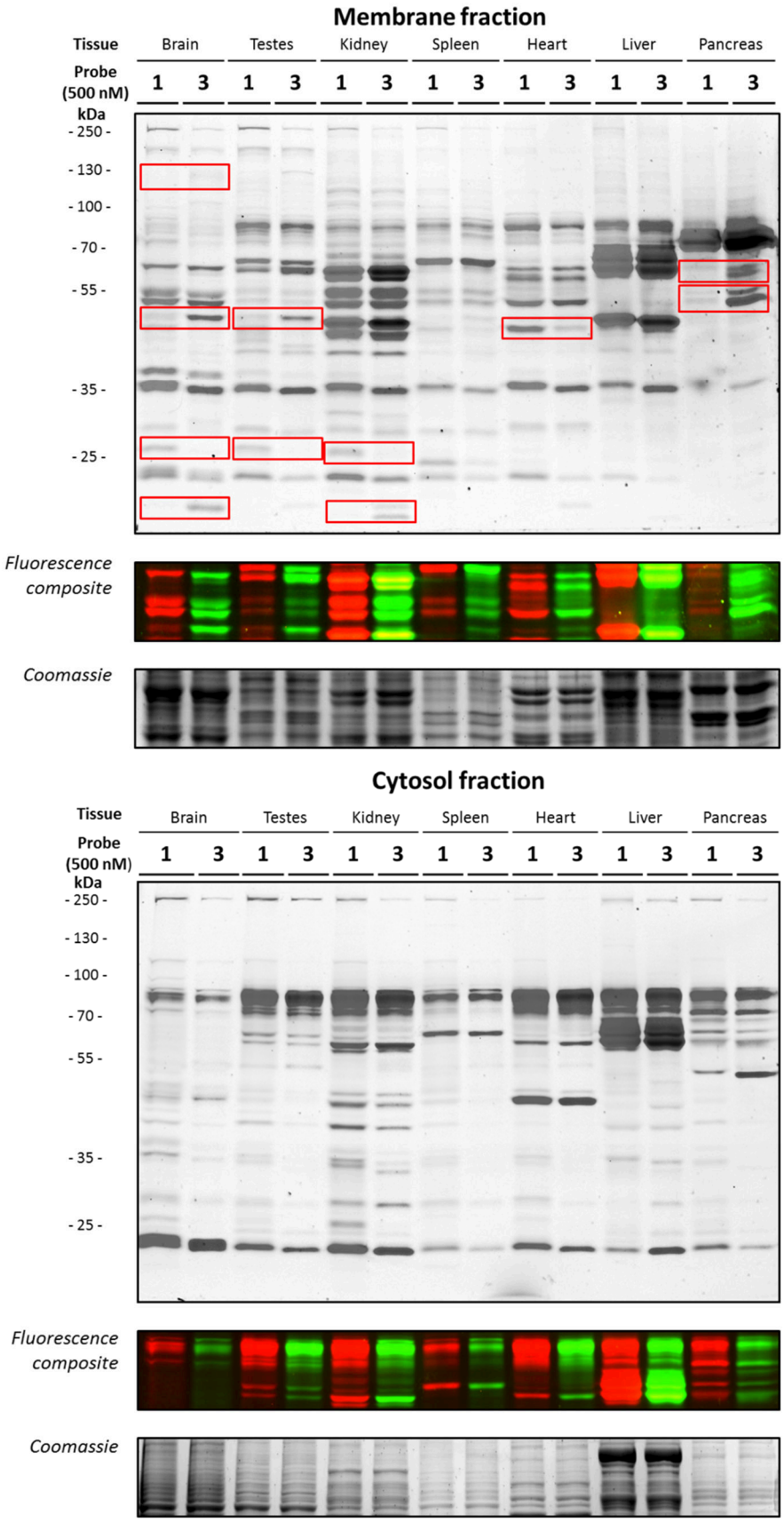

Figure 6.2 | Direct comparison of FP-TAMRA (**1**) and FP-BODIPY (**3**) labeling patterns of seven mouse tissue lysates. Red boxes highlight strong differences between the two fluorescent probes.

Detailed profiling of the fluorophosphonate probes **1**, **3** and **4**

Brain lysates were selected for further profiling of probe **1** and **3**, as well as control probe **4**, because the brain is the most studied target organ for ECS modulation. In an initial screen, the three ABPs were incubated with both brain membrane and soluble proteomes (Figure 6.3A, Figure S6.2). While the labeling profile in the soluble proteome was not significantly different between the three probes, FP-BODIPY (**3**) labeled various proteins at lower concentrations in the membrane proteome. To determine the half maximum effect (EC_{50}) values of serine hydrolase labeling in the membrane proteome, the probes were dosed at a wide range of concentrations (10 pM - 10 µM) and the fluorescent signal of 18 distinct bands was quantified and corrected for protein loading by coomassie staining (Figure S6.2 and S6.3). To study the effect of fluorophore and linker length on serine hydrolase labeling by FP-probes in mouse brain membrane proteome, the change in pEC_{50} of ABP **3** and **4** relative to ABP **1** was calculated (Figure 6.3B and Table S6.1). The increased linker length did not significantly alter the labeling efficiency for FP-TAMRA for most proteins, except for fatty acid amide hydrolase (FAAH) (left plot, Figure 6.3C), whereas the change in fluorophore led to a 10-fold increased potency in labeling for several proteins (3, 8 and 18). Of note, FAAH labeling was already visualized at 10 nM FP-BODIPY **3** and DAGL-α (band 3) at 500 nM (Figure 6.3C, A, respectively). The third plot in Figure 6.3B, comparing probe **3** and **4**, which only differ in reporter tag, shows that almost all the difference between the commercial FP-TAMRA probe **1** and the newly synthesized FP-BODIPY probe **3** observed in the central plot is due to the change in fluorophore. The most likely explanation for the observed potency increase when changing from TAMRA to BODIPY-FP is the strong increase in lipophilicity. The CLogP of BODIPY-FL is 3.7 points higher than that of TAMRA, which would make it more favourable to stick to proteins and membranes, possibly causing a higher local concentration and thus better labeling. This explanation is in line with the observation that the strongest differences are observed in the membrane fractions, and, between organs, in the brain. Finally, the impact of the addition of a reporter tag was visualized by pre-incubation with 'dark' alkyne-FP (**5**) (Figure 6.4). This competitive labeling shows that alkyne-FP only completely prevented labeling by the fluorescent probes at 5-10 µM, demonstrating the significantly reduced affinity of the fluorophosphonate inhibitor when lacking the reporter tag. All together, these data demonstrate that the choice of fluorophore influences the labeling efficiency of FP-based probes.

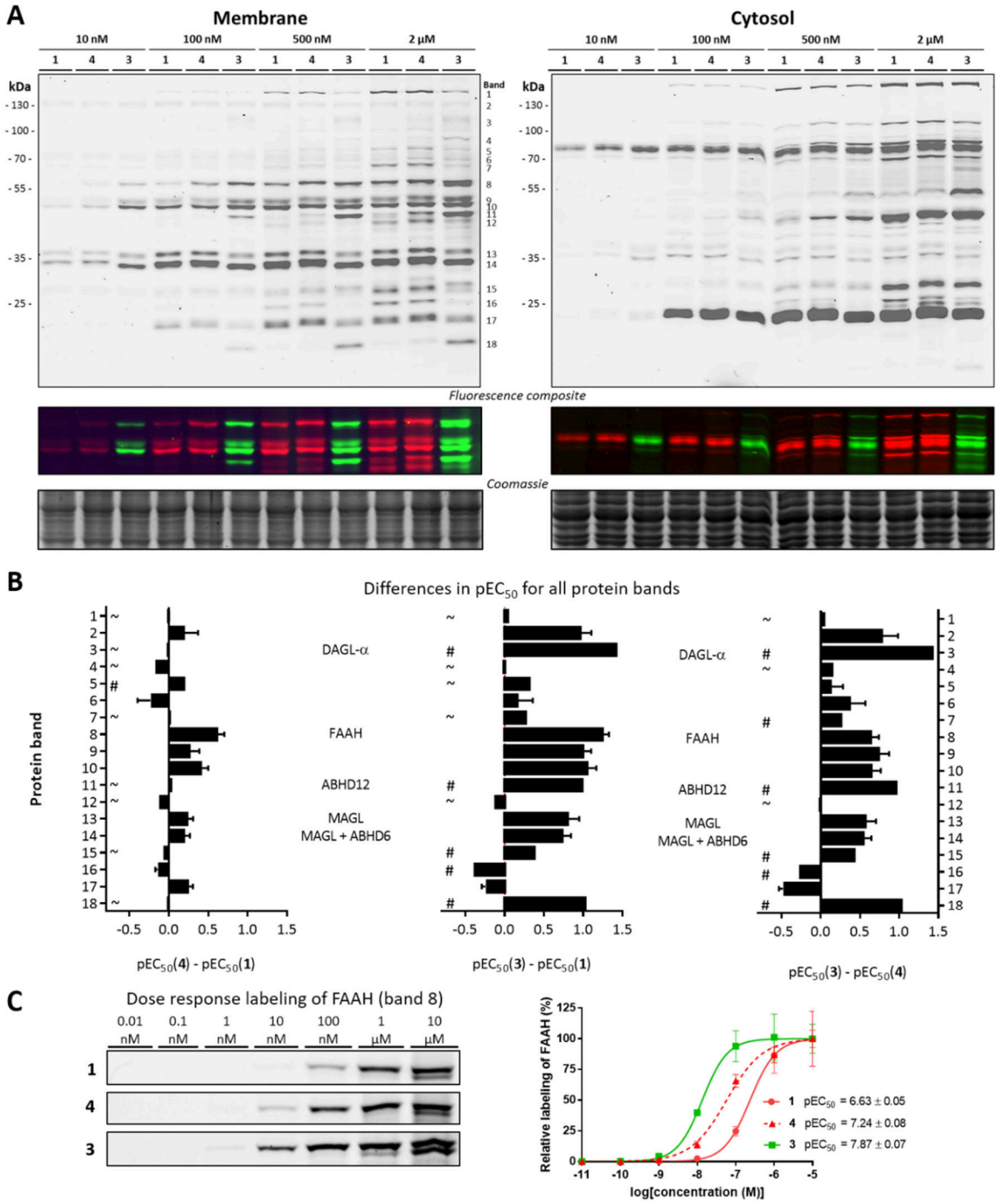

Figure 6.3 | Concentration dependent labeling of probes **1**, **3,** and **4**. A) Four doses of the FP probes label mouse brain proteome in a distinct pattern with different affinities. B) Quantified affinity-differences among the evaluated FP-probes for the 18 bands denoted in A. # indicates a $pEC_{50} \leq 6$ for one of the two probes, meaning that the difference is most likely greater than the given value. ~ indicates a $pEC_{50} \leq 6$ for both probes, meaning that both probes label these proteins only at high concentrations. All quantifications assumed 100% labeling of protein at 10 µM probe. C) Example of the labeling pattern of band 8 (FAAH) and corresponding pEC_{50} curves and values. DAGL-α: diacylglycerol lipase α, ABHD12, ABHD6: α/β hydrolase domain containing protein 12, 6, MAGL: monoacylglycerol lipase, FAAH: fatty acid amide hydrolase.

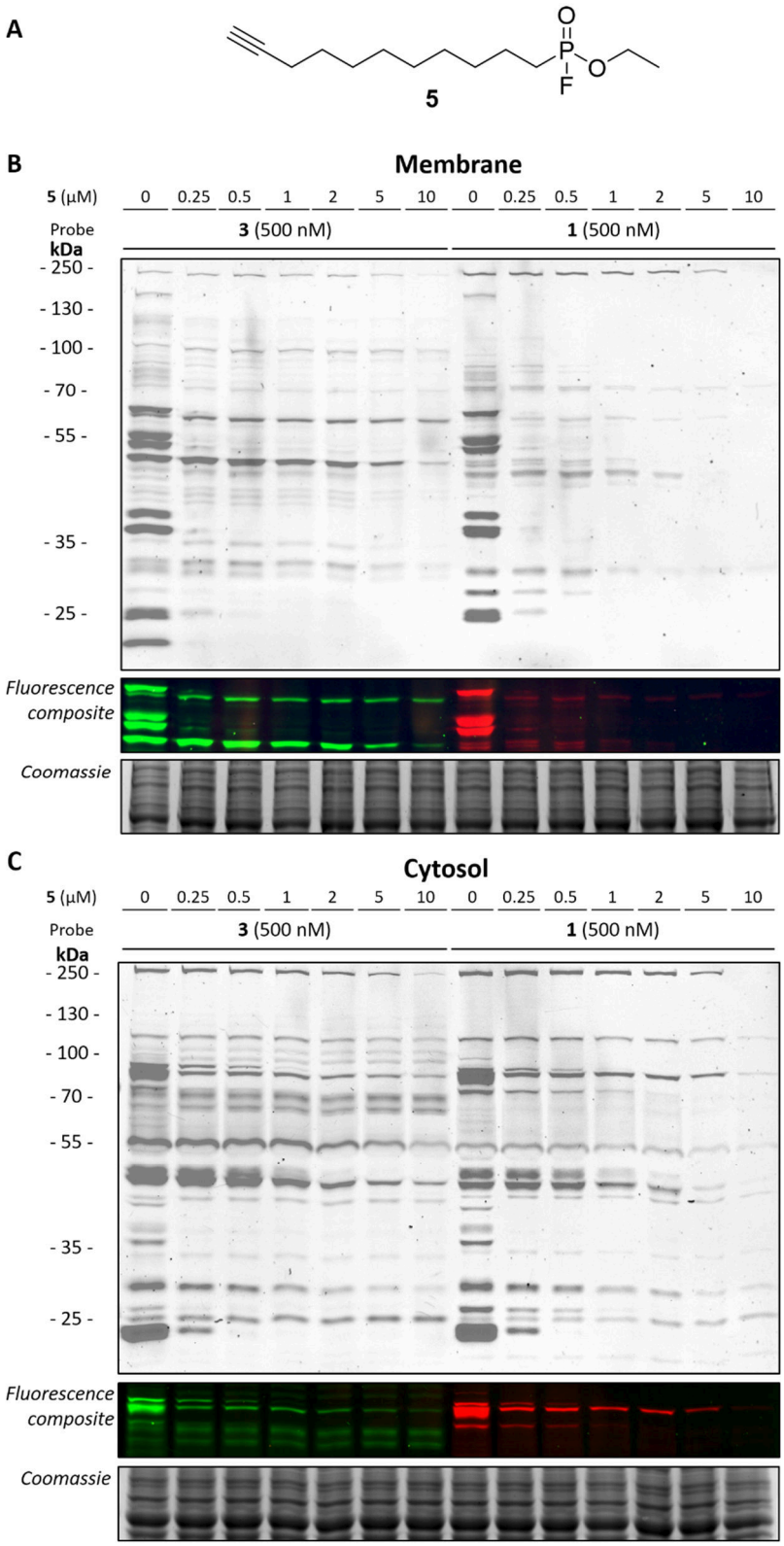

Figure 6.4 | Dose response inhibition of probe **1** and **3** by 'dark' alkyne-FP (**5**). A) Structure of alkyne-FP (**5**) B) Mouse brain membrane proteome was incubated with **5** in increasing dose to prevent labelling by probe **1** and **3**. C) As B) but utilizing mouse brain cytosolic proteome. The Figure is a grey scale composite of two channels. Fluorescence composite is included, green for probe **3** and red for probe **1**. Coomassie is shown as protein loading control.

Next, it was tested whether the activity and selectivity profile of serine hydrolase inhibitors would be dependent on the reporter group of the activity-based probe. To this end, a covalent irreversible FAAH inhibitor, PF-04457845[14], and a reversible inhibitor, LEI104[9] (Figure 6.5), were tested in a competitive ABPP setting using probe **1** (500 nM) and probe **3** (500 and 10 nM) (Figure 6.6A). Importantly, the pIC_{50} values of both inhibitors were not dependent on the fluorescent reporter group of the probe, nor the probe concentration. This indicated that FP-BODIPY **3** can be used in a drug discovery setting to profile inhibitor activity using ABPP.

Development of a multiplexed assay

Having developed two complementary probes (FP-BODIPY (**3**) and MB064) with different reporter groups and distinct labeling patterns, it was tested whether they can be used in a multiplexed ABPP assay to profile the activity and selectivity of compounds inhibiting biosynthetic or catabolic enzymes of the ECS.[6,7,15] To this end, a cocktail of FP-BODIPY **3** (10 nM) and MB064 **2** (250 nM) was used to label mouse brain membrane proteomes. This enabled the simultaneous visualization and quantification of DAGL-α, DDHD2, α/β hydrolase domain containing protein 16a (ABHD16a), FAAH, monoacylglycerol lipase (MAGL), ABHD6 and ABHD12 activities in a single experiment (Figure 6.6B). Bands were identified based on previous studies.[9,16] Phopholipase 2 group IV E (PLA2G4E) and ABHD4 can be labeled by FP-BODIPY and MB064, respectively, but their endogenous expression in brain is too low to be visualized.[17] A panel of inhibitors consisting of JZL184 (MAGL)[18], DH376 (DAGL-α, ABHD6)[15], THL (DAGL-α, ABHD6, ABHD12, ABHD16a, DDHD2)[19], PF-04457845 (FAAH)[14], LEI104 (DAGL-α, FAAH)[9] and LEI105 (DAGL-α)[16] (Figure 6.5) was used to confirm the identity of each fluorescent band (Figure 6.6B). As a final validation, the inhibitory activities of LEI104 on DAGL-α and FAAH were confirmed in this new multiplexed ABPP assay and were found to be in line with previously reported data (Figure 6.6C).[9]

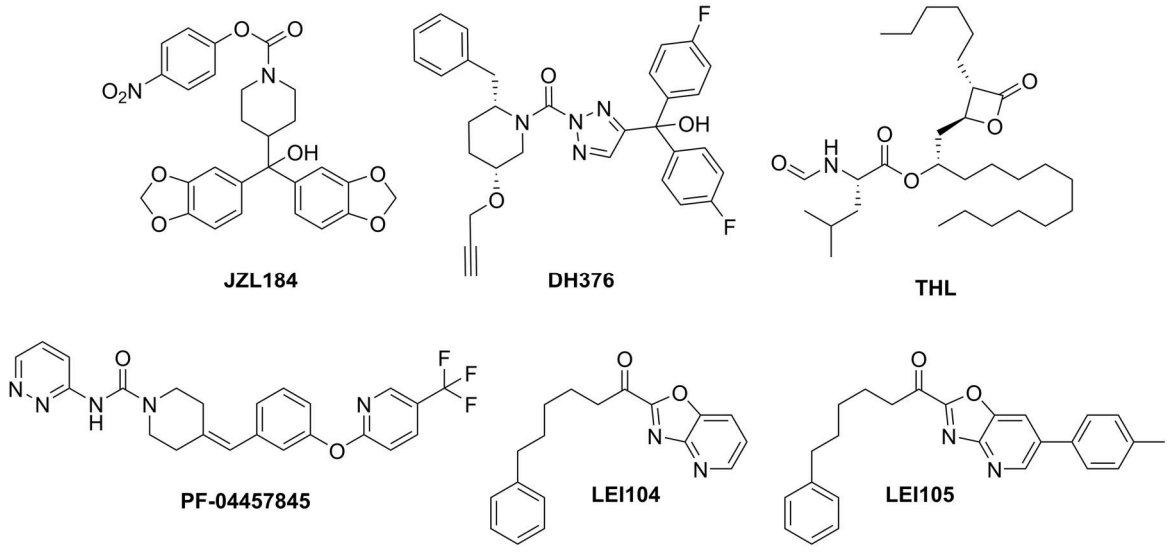

Figure 6.5 | Structures of endocannabinoid serine hydrolase inhibitors used in Figure 6.6.

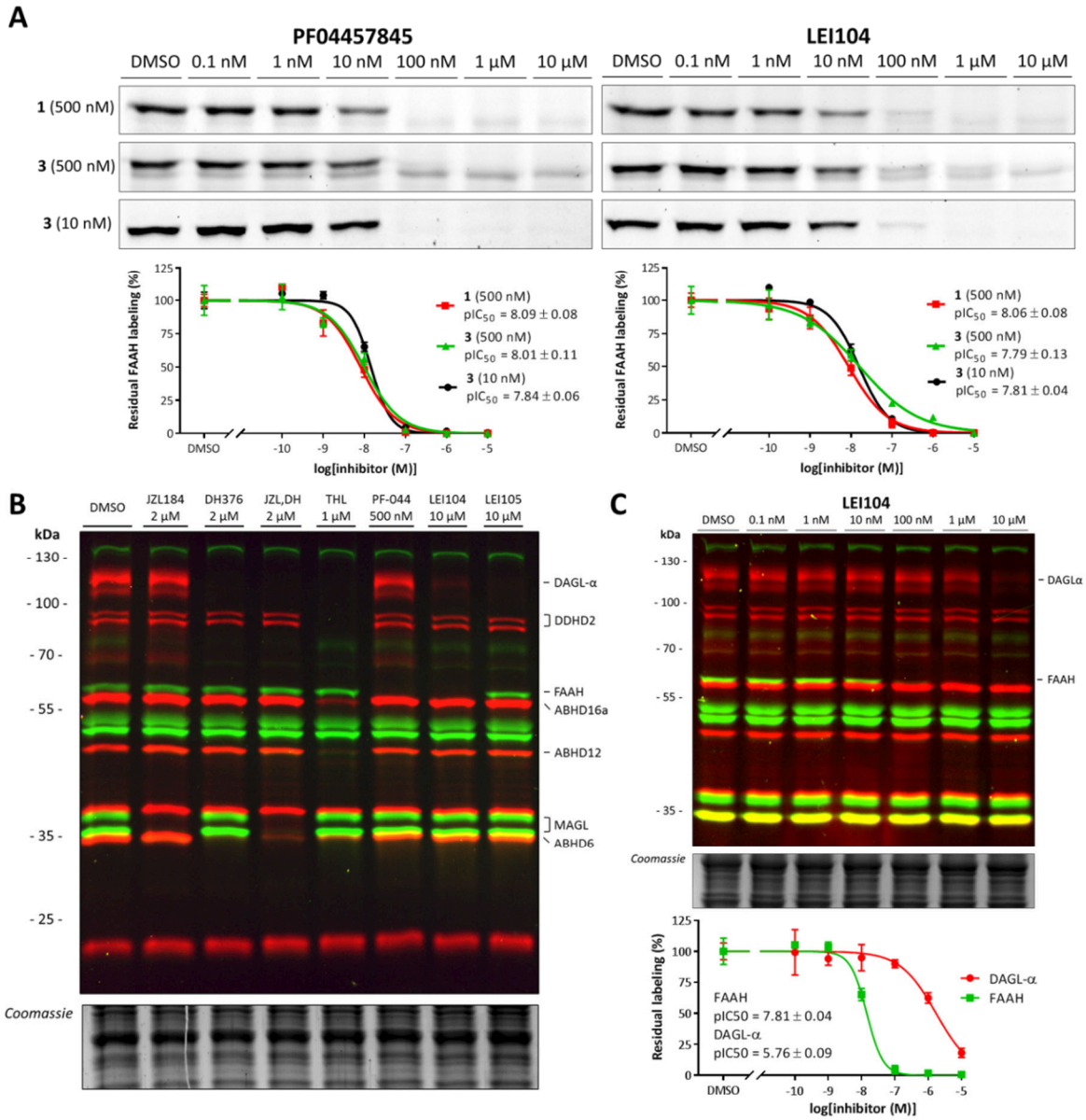

Figure 6.6 | Illustration of the applicability of the prepared probe cocktail. A) Dose response inhibition of FAAH using PF-04457845, covalent irreversible, and LEI104, reversible, to test the dependency of the pIC_{50} determination on probe affinity and concentration. No statistical significant differences have been found between the probe pairs ($p > 0.05$, Two-sided Student's *t*-test). B) Six inhibitors targeted for different endocannabinoid serine hydrolases were shown to inhibit their specific targets using the probe cocktail. C) Dose response inhibition with LEI104 shows, in one gel, the inhibition of DAGL-α and FAAH. Quantification shows agreement of the pIC_{50} with literature values.[9]

The validated assay was employed to study the selectivity and activity of two MAGL inhibitors. First the recently published β-lactam based MAGL inhibitor NF1819 (**6**) was tested (Figure 6.7A), which was active in several animal models of multiple sclerosis, pain and predator stress-induced long-term anxiety.[20,21] The target-interaction profile of NF1819 (**6**) was compared to the experimental drug ABX-1431 (**7**), currently in phase 2 clinical trials for the treatment of Tourette Syndrome.[22–24] To this end, they were incubated at various concentrations with mouse brain membrane proteome (Figure 6.7B, 6.7C and Figure S6.4). Inhibition of MAGL was confirmed with a pIC_{50} of 8.1 ± 0.1 for **6** and 6.7 ± 0.1 for **7** (Figure 6.7D, 6.7F), in accordance with previously published data.[20,22] Of note, for **6** various off-targets were observed, including ABHD6, LYPLA and an unidentified protein (Figure 6.7E). ABHD6 was inhibited at equal potency, whereas LYPLA demonstrated a 50-fold lower potency. FAAH labeling was only slightly reduced at concentrations > 10 µM. The target-interaction landscape of **7** is clean, even at 10 µM no clear off-targets were observed. The relatively small selectivity window of **6** over ABHD6 should be taken into account during the biological evaluations of this inhibitor as it may contribute to the rise of 2-AG levels.

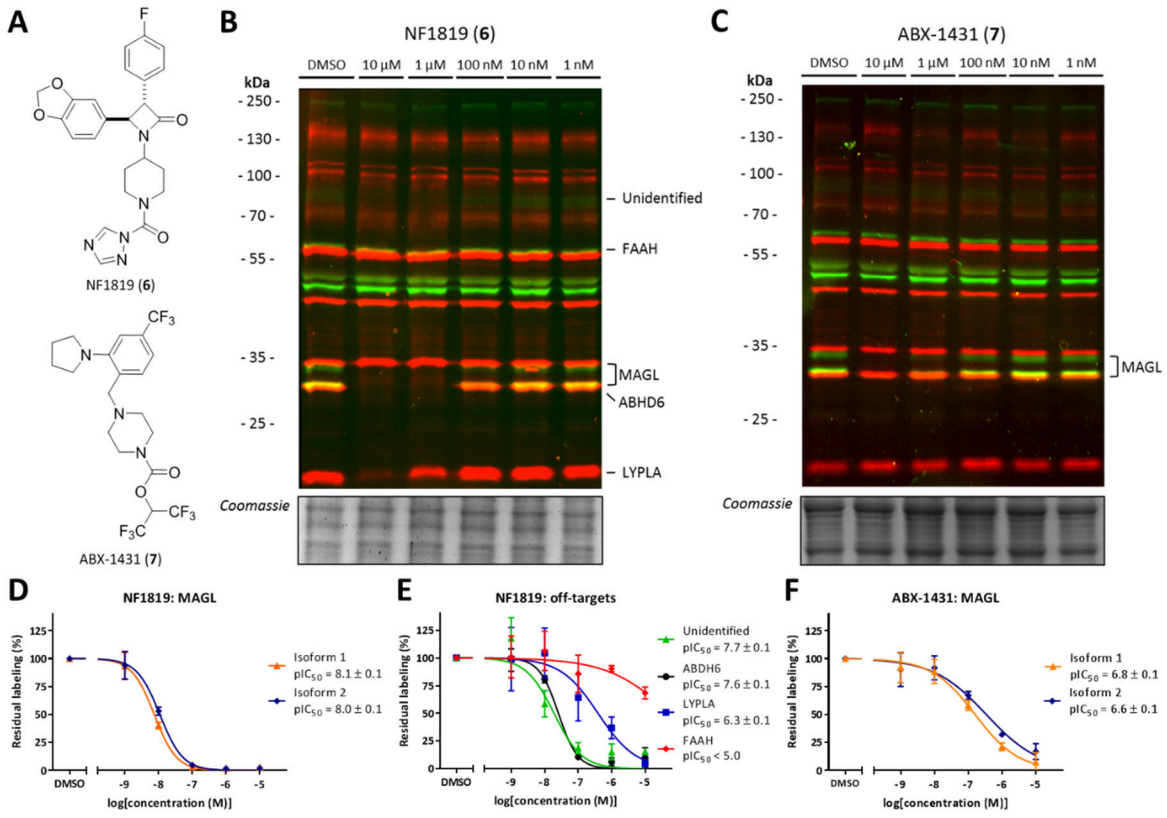

Figure 6.7 | Off-target profiling of β-lactam based MAGL inhibitor (**6**) and clinical candidate ABX-1431 (**7**) in mouse brain membrane proteome. A) Chemical structure of (**6**) and (**7**). B) Dose response inhibition with (**6**) shows several off-targets in mouse brain membrane. C) Dose response inhibition with (**7**) shows selective MAGL inhibition in mouse brain membrane. D) pIC_{50} curves and values of (**6**) against MAGL. E) pIC_{50} curves and values of (**6**) against its off-targets. F) pIC_{50} curves and values of (**7**) against MAGL.

Conclusion

In conclusion, FP-BODIPY (**3**) was synthesized and characterized as a new ABP, extending the chemical toolbox to study serine hydrolase activity in native biological samples. The choice of fluorophore was found to be of great influence on labeling patterns, even for broadly reactive probes such as fluorophosphonates. This finding should be taken into account when designing ABPs. FP-BODIPY (**3**) in conjunction with MB064 (**2**) was used to develop a multiplexed ABPP assay, which was validated by profiling inhibitor activity and selectivity on a broad range of endocannabinoid hydrolases in mouse brain tissue in a single experiment. This multiplexed ABPP assay was then applied to investigate the specificity of a recently published *in vivo* active MAGL inhibitor and an experimental drug currently going through clinical trials.

Methods

Materials

The inhibitors JZL184, PF-04457845 and tetrahydrolipstatin were commercially available (Sigma Aldrich). The syntheses of DH376, LEI104, LEI105, NF1819 and ABX-1431 were previously described.[9,15,16,20,23]

Tissue preparation

Organs were isolated from mice following standard guidelines as approved by the ethical committee of Leiden University (DEC#13191). Isolated organs were frozen in liquid nitrogen and stored at -80 °C. Organs were thawed on ice and homogenized by a glass stick douncing homogenizer in cold lysis buffer (20 mM HEPES, pH 7.2, 2 mM DTT, 1 mM $MgCl_2$, 2.5 U/mL benzonase). The resulting suspension was centrifuged at 1500 rpm for 5 minutes at 4 °C to get rid of residual solid tissue. The supernatant was centrifuged 45 minutes at 93,000 *g* at 4 °C to separate soluble (cytosol) and insoluble (membrane) fractions. The pellet (membrane) was resuspended in storage buffer (20 mM HEPES, pH 7.2, 2 mM DTT) using an insulin syringe. The protein concentration was measured using a Qubit™ protein assay and was adjusted to 2 mg/mL using storage buffer. The resulting lysates were frozen in liquid nitrogen and stored at -80 °C for later use.

Activity-based protein profiling

Lysate (19 µL, 2 µg/µL) was thawed on ice. For comparative ABPP (one probe and no inhibitor), 1 µL of probe (20x stock in DMSO) was added to the sample, vortexed briefly and incubated for 15 minutes at RT. For competitive ABPP (one inhibitor and one probe), 0.5 µL of the inhibitor (40x stock in DMSO) or pure DMSO (as vehicle) was added to the sample, vortexed briefly and incubated for 20 minutes at RT (37 °C for Figure 6.6A and C to compare with literature values). Subsequently, 0.5 µL probe (40x stock in DMSO) was added to the proteome sample, vortexed briefly and incubated for 15 minutes at RT. Final volume was 20 µL (5% DMSO). The reaction was quenched by the addition of 7.5 µL of 4*Laemmli-buffer (final concentrations: 60 mM Tris (pH 6.8), 2% (w/v) SDS, 10% (v/v) glycerol, 1.25% (v/v) β-mercaptoethanol, 0.01% (v/v) bromophenol blue). 9 µL (12 µg protein) of quenched reaction mixture was resolved on 10% acrylamide SDS-PAGE (180 V, 75 min). Fluorescence was measured using a Biorad ChemiDoc MP system (fluorescence channels Cy2, Cy3, Cy5). Gels were then stained using coomassie staining and imaged for protein loading control.

Labeling quantification

Fluorescence quantification was performed using Imagelab 6.0 (Biorad). Intensities were normalized to 10 µM (for Figure 6.3) or DMSO control (Figure 6.6 and 6.7) and corrected for protein loading by coomassie staining. pEC_{50} values were calculated using GraphPad Prism 7. For all pEC_{50} determinations three replicates of each condition were used.

Statistical methods

Two-sided Student's *t*-tests were performed using GraphPad Prism 7.0 with the standard Holm-Šídák method to correct for multiple comparisons.

Synthetic methods

General remarks

Reagents were purchased from Sigma Aldrich, Alfa Aesar, AnaSpec or ACROS organics at reagent grade and used without further purification. All moisture sensitive reactions were performed under a nitrogen atmosphere. All solvents were dried using molecular sieves. Ethyl acetate was distilled before use. Glassware was oven dried prior to use. ^{1}H and ^{13}C NMR spectra were recorded on a Bruker DPX-300 (300 MHz), AV-400 (400 MHz) or Bruker DRX-500 (500 MHz). Used software for interpretation of NMR-data was Bruker TopSpin 1.3 and MestreNova 11.0. Chemical shift values are reported in ppm with tetramethylsilane or solvent resonance as the internal standard ($CDCl_3$: δ 7.26 for ^{1}H, δ 77.16 for ^{13}C). ^{31}P-NMR shifts are given in ppm relative to phosphoric acid. ^{19}F-NMR shifts are given in ppm relative to $CFCl_3$. Data are reported as follows: chemical shifts (δ), multiplicity (s = singlet, d = doublet, dd = double doublet, td = triple doublet, t = triplet, q = quartet, bs = broad singlet, m = multiplet), coupling constants *J* (Hz), and integration. Liquid chromatography analysis was performed on a Finnigan Surveyor LC/MS system, equipped with a C18 column. Flash chromatography was performed using SiliCycle silica gel type SiliaFlash P60 (230–400 mesh). TLC analysis was performed on Merck silica gel 60/Kieselguhr F254, 0.25 mm. Compounds were visualized using $KMnO_4$

stain (K_2CO_3 (40 g), $KMnO_4$ (6 g), and water (600 mL)) or CAM stain ($Ce(NH_4)_4(SO_4)_4{\cdot}2H_2O$ (ceric ammonium sulfate: 10.0 g); ammonium molybdate (25 g); conc. H_2SO_4 (100 mL); H_2O (900 mL)). High resolution mass spectra (HRMS) were recorded by direct injection on a q-TOF mass spectrometer (Synapt G2-Si) equipped with an electrospray ion source in positive mode with Leu-enkephalin (*m/z* = 556.2771) as an internal lock mass. The instrument was calibrated prior to measurement using the MS/MS spectrum of Glu-1-fibrinopeptide B.

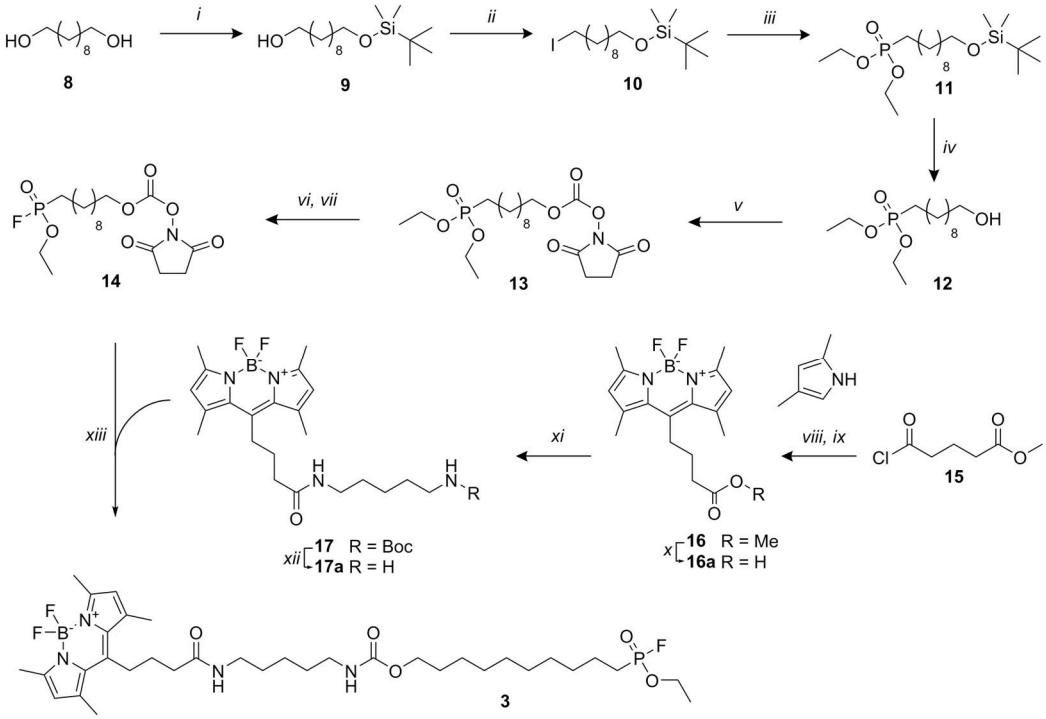

Scheme S6.1 | Synthesis of probe **3**. Reagents and conditions: *i*) TBDMS-Cl, DMAP, imidazole, DMF, RT, 42%; *ii*) I_2, triphenylphosphine, THF, RT, 93%; *iii*) $POEt_3$, reflux, 99%; *iv*) TBAF, THF, 0 – 20 °C, 86%; *v*) disuccinylcarbonate, triethylamine, DMF, RT, 91%; *vi*) oxalyl chloride, DCM, RT; *vii*) DAST, DCM, -78 °C, 46%; *viii*) DCM, reflux; *ix*) triethylamine, $BF_3{\cdot}OEt_2$, DCM, toluene, 50 °C, 46%; *x*) NaOH, H_2O, THF, RT, 82%; *xi*) *N*-Boc-cadaverine, EDC·HCl, HOBt, triethylamine, DCM, RT, 56%; *xii*) TFA, DCM, RT, 41%; *xiii*) triethylamine, DCM, DMF, RT, 26%.

10-*tert*-Butyldimethylsilane-1-decanol (**9**)

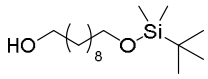

8 (10.3 g, 57.4 mmol), imidazole (3.91 g, 57.4 mmol) and 4-(dimethylamino)-pyridine (80 mg, 0.65 mmol) were dissolved in dry DMF at RT. Subsequently, *tert*-butyl dimethyl silyl chloride (4.45 g, 28.8 mmol) was added and the mixture was stirred at RT for 5 hours. The mixture was quenched with saturated $NaHCO_3$ (200 mL, aq.) and H_2O (200 mL). The mixture was extracted with EtOAc (3x 200 mL) and the organic layers were combined and dried ($MgSO_4$), filtered and evaporated to afford the crude product as a white solid. Purification was performed using column chromatography (5% to 20% EtOAc in pentane). Pure fractions were combined and evaporated to dryness to afford the title compound (3.52 g, 12.1 mmol, 42%). ^{1}H NMR (300 MHz, $CDCl_3$) δ 3.69 – 3.49 (m, 4H), 1.64 – 1.42 (m, 5H), 1.37 – 1.21 (m, 12H), 0.88 (s, 9H), 0.03 (s, 6H). ^{13}C NMR (75 MHz, $CDCl_3$) δ 63.47, 63.14, 32.99, 32.92, 29.68, 29.55, 26.11, 25.91, 25.87, 18.51, -5.13.

10-Iododecyloxy-1-(*tert*-butyl)dimethylsilane (**10**)

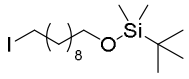

Triphenylphosphine (3.5 g, 13 mmol) and imidazole (1.8 g, 26 mmol) were dissolved in THF (62 mL). Subsequently, iodine (3.5 g, 14 mmol) was slowly added to the solution. The mixture was stirred for 20 minutes at RT under inert atmosphere. Then, **9** (3.5 g, 12 mmol) dissolved in THF (14 mL) was slowly added to the stirred solution. The solution turned brown/red. During the reaction, a yellow precipitate formed. The reaction was allowed to stir at RT for 1 hour. The volatiles were evaporated and the residue was taken up in an emulsion of Et_2O (100 mL) and sodium thiosulfate (100 mL, 10%, aq.). The yellow colour disappeared after the addition of the thiosulfate. The organic layer was washed with water and with brine. The organic layer was dried ($MgSO_4$), filtered, and the solvent evaporated to afford white crystals. Purification was done using silica column chromatography (1% Et_2O in pentane), affording the

title compound as a colourless oil (4.31 g, 11.3 mmol, 93%). ^{1}H NMR (300 MHz, $CDCl_3$) δ 3.60 (t, *J* = 6.6 Hz, 2H), 3.19 (t, *J* = 7.0 Hz, 2H), 1.82 (p, *J* = 7.0 Hz, 2H), 1.56 – 1.44 (m, 2H), 1.44 – 1.22 (m, 12H), 0.89 (s, 9H), 0.06 (s, 6H). ^{13}C NMR (75 MHz, $CDCl_3$) δ 63.46, 33.72, 33.02, 30.65, 29.66, 29.51, 28.68, 26.14, 25.93, 7.49, -5.09.

Diethyl 10-(*tert*-butyldimethylsiloxy)decylphosphonate (**11**)

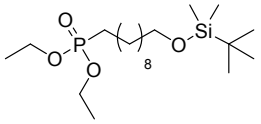

10 (4.31 g, 11.3 mmol) was dissolved in triethylphosphite (10 mL, 58 mmol). The solution was then heated to 155 °C under reflux conditions for 5 hours under inert atmosphere. The resulting solution was then concentrated under reduced pressure to afford the title compound as a light yellow oil (4.4 g, 11 mmol, 99%). ^{1}H NMR (300 MHz, $CDCl_3$) δ 4.21 – 3.98 (m, 4H), 3.59 (t, *J* = 6.6 Hz, 2H), 1.84 – 1.18 (m, 24H), 0.89 (s, 9H), 0.06 (s, 6H).

Diethyl 10-hydroxydecylphosphonate (**12**)

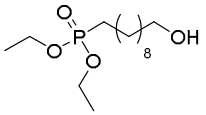

To a cooled (0 °C) solution of **11** (4.4 g, 11 mmol) in dry THF (40 mL), TBAF (12.3 mL, 1 M in THF) was slowly added under inert atmosphere. The reaction was allowed to stand overnight while warming up to RT. The reaction mixture was concentrated and dissolved in 100 mL DCM and washed twice with water (50 mL) and with brine (50 mL). The organic layer was dried ($MgSO_4$), filtered, and concentrated. The resulting yellow oil was purified using column chromatography (5% MeOH in DCM) to afford the title compound as a light yellow oil (2.84 g, 9.65 mmol, 86%). ^{1}H NMR (300 MHz, $CDCl_3$) δ 4.23 – 3.95 (m, 4H), 3.64 (t, *J* = 6.5 Hz, 2H), 1.88 – 1.46 (m, 9H), 1.46 – 1.18 (m, 16H). ^{13}C NMR (126 MHz, $CDCl_3$) δ 62.98, 61.50 (d, *J* = 6.6 Hz), 32.87, 30.64 (d, *J* = 16.8 Hz), 29.56, 29.45, 29.34, 29.12, 25.82, 25.74 (d, *J* = 140.4 Hz), 22.44 (d, *J* = 5.2 Hz), 16.56 (d, *J* = 6.0 Hz). ^{31}P NMR (202 MHz, $CDCl_3$) δ 33.26.

10-(Diethoxyphophoryl) decyl-1-succinimidyl carbonate (**13**)

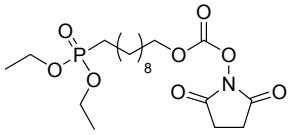

12 (189 mg, 0.64 mmol) was dissolved in 5 mL dry DMF and TEA (0.20 mL, 1.4 mmol) was added. To the stirred solution *N,N'*-disuccinimidyl carbonate (328 mg, 1.28 mmol) was added. The solution was stirred for 40 hours under argon atmosphere at RT. The resulting mixture was taken up in an emulsion of water (20 mL) and EtOAc (20 mL) and stirred for 10 minutes. Then, H_2O (50 mL) was added. The layers were separated and the aqueous layer was extracted using EtOAc (3x 20 mL). The combined organic layers were washed with brine, dried ($MgSO_4$), filtered and concentrated. Purification was performed using silica chromatography (5% MeOH in DCM) to afford **13** as a light yellow oil (254 mg, 0.58 mmol, 91%). ^{1}H NMR (300 MHz, $CDCl_3$) δ 4.32 (t, *J* = 6.7 Hz, 2H), 4.18 – 4.01 (m, 4H), 2.84 (s, 4H), 1.81 – 1.65 (m, 4H), 1.65 – 1.51 (m, 2H), 1.46 – 1.21 (m, 18H). ^{13}C NMR (75 MHz, $CDCl_3$) δ 168.82, 71.74, 61.49 (d, *J* = 6.5 Hz), 30.68 (d, *J* = 17.1 Hz), 29.40, 29.33, 29.13, 28.44, 25.77 (d, *J* = 140.1 Hz), 25.57, 25.50, 22.50 (d, *J* = 5.2 Hz), 16.59 (d, *J* = 6.0 Hz).

10-(Ethoxyfluorophophoryl) decyl-1-succinimidyl carbonate (**14**)

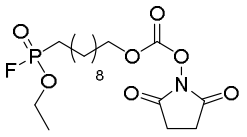

13 (254 mg, 0.58 mmol) was dissolved in 3 mL DCM. Subsequently, oxalyl chloride (0.54 mL, 6.2 mmol) was added and the reaction was stirred for 16 hours at room temperature under N_2-atmosphere. The reaction mixture was diluted with DCM (10 mL), then quenched with water (10 mL). The mixture was stirred for 15 minutes. The layers were separated and the aqueous layer was extracted using DCM and EtOAc (2x). The combined organic layers were dried ($MgSO_4$), filtered and concentrated. The residue was dissolved in DCM (3 mL), placed under N_2-atmosphere and cooled down to -78 °C. Slowly, diethylaminosulfur trifluoride (0.19 mL, 1.4 mmol) was added. The reaction was stirred for 30 minutes at -78 °C. The reaction was quenched with water (5 mL) and EtOAc (5 mL) and warmed up to room temperature. The layers were separated and the aqueous layer was extracted using EtOAc. The combined organic layers were dried ($MgSO_4$), filtered and concentrated *in vacuo* to afford the crude product. Purification was performed with column chromatography (50% EtOAc in pentane) to afford the title compound as a slightly yellow oil (109 mg, 0.27 mmol, 46%). R_f (50% EtOAc in pentane) = 0.4. ^{1}H NMR (500 MHz, $CDCl_3$) δ 4.32 (t, *J* = 6.7 Hz, 2H), 4.29 – 4.18 (m, 2H), 2.84 (s, 4H), 1.95 – 1.83 (m, 2H), 1.81 – 1.71 (m, 2H), 1.71 – 1.58 (m, 2H), 1.45 – 1.35 (m, 7H), 1.35 – 1.21 (m, 8H). ^{13}C NMR (126 MHz, $CDCl_3$) δ 168.83, 151.73, 71.75, 63.15 (d, *J* = 7.3 Hz), 30.37 (d, *J* = 16.9 Hz), 29.37, 29.24, 29.10, 29.01, 28.45, 25.59, 25.50, 24.41 (dd, *J* = 143.0, 22.2 Hz), 22.01 (d, *J* = 5.6 Hz), 16.47 (d, *J*

= 5.6 Hz). ^{31}P NMR (202 MHz, $CDCl_3$) δ 32.52 (d, *J* = 1070 Hz). ^{19}F NMR (471 MHz, $CDCl_3$) δ -65.03 (d, *J* = 1070 Hz).

4-(4,4-Difluoro-1,3,5,7-tetramethyl-4-bora-3a,4a-diaza-s-indacene-8-yl)-butyric methyl ester (BODIPY-butyric methyl ester) (**16**)

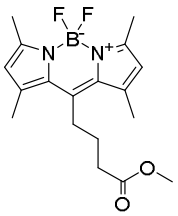

2,4-Dimethylpyrrole (716 mg, 7.3 mmol) was dissolved in DCM (30 mL) and placed under argon atmosphere. Then, methyl 5-chloro-5-oxopentanoate **15** (0.68 mL, 4.9 mmol) was added to the solution. The mixture was refluxed for 2 hours. TEA (3.5 mL, 25 mmol) was dissolved in toluene (20 mL) and was added to the solution. Subsequently, borontrifluoride etherate (4.1 mL, 33 mmol) was added and the solution was heated to 50 °C for 1.5 hours. The mixture was diluted with DCM. The solution was quenched with HCl (1 M, aq.) and water. The layers were separated and the organic layer was washed with HCl (1 M, aq.). The combined aqueous layers were extracted three times with DCM. The combined organic layers were dried ($MgSO_4$), filtered and concentrated. Purification was performed using silica column chromatography (gradient of 10% – 20 % EtOAc in pentane). The product was obtained as a red/brown solid (777 mg). NMR showed presence of TEA·HCl, making up for 25%$_{wt}$, as calculated by NMR-integrals. The resulting crude was used in subsequent reactions without further purification (584 mg, 1.68 mmol, 46%). ^{1}H NMR (300 MHz, $CDCl_3$) δ 6.06 (s, 2H), 3.70 (s, 3H), 3.10 – 2.91 (m, 2H), 2.57 – 2.34 (m, 14H), 2.03 – 1.86 (m, 2H).

4-(4,4-Difluoro-1,3,5,7-tetramethyl-4-bora-3a,4a-diaza-s-indacene-8-yl)-butyric acid (**16a**)

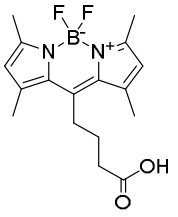

16 (285 mg, 0.82 mmol) was dissolved in THF (5 mL). NaOH (4 mL, 2M, aq.) and water (3 mL) were added to the solution. The reaction mixture was stirred 16 hours at room temperature under inert atmosphere. The mixture was acidified using HCl (6 mL of 2 M aq.) and HCl (1 mL 37%$_{wt}$ aq.). The resulting mixture was extracted twice with EtOAc. The combined organic layers were dried ($MgSO_4$), filtered and concentrated. Purification was performed using column chromatography (5% AcOH and 15% EtOAc in pentane) to afford the title compound as a red solid (225 mg, 0.67 mmol, 82%). R_f (15:4:1 pentane:EtOAc:AcOH) = 0.3. ^{1}H NMR (400 MHz, $CDCl_3$) δ 9.10 (s, 1H), 6.05 (s, 2H), 3.07 – 2.95 (m, 2H), 2.55 (t, *J* = 7.2 Hz, 2H), 2.51 (s, 6H), 2.41 (s, 6H), 2.01 – 1.90 (m, 2H). ^{13}C NMR (101 MHz, $CDCl_3$) δ 178.81, 154.36, 144.85, 140.52, 131.55, 121.96, 34.27, 27.50, 26.63, 16.43, 14.60.

tert-Butyl (5-(4-BODIPY-butanamido)pentyl)carbamate (**17**)

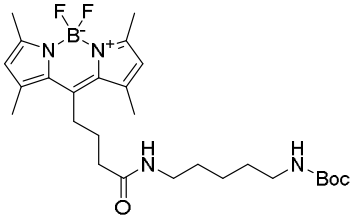

16a (225 mg, 0.67 mmol) was dissolved in DCM (30 mL), to which EDC·HCl (227 mg, 1.29 mmol), TEA (0.30 mL, 2.1 mmol), *N*-Boc cadaverine (0.25 mL, 1.22 mmol) and HOBt (106 mg, 0.78 mmol) were added. The reaction was stirred for 56 hours at room temperature. The reaction was quenched with HCl (20 mL, 0.1 M, aq.) and extracted using DCM. The combined organic layers were dried ($MgSO_4$), filtered and concentrated. Purification using column chromatography (70% EtOAc in pentane) afforded the title compound as an orange solid (206 mg, 0.397 mmol, 56%). ^{1}H NMR (400 MHz, $CDCl_3$) δ 6.05 (s, 2H), 5.77 (s, 1H), 4.60 (s, 1H), 3.27 – 3.19 (m, 2H), 3.11 (q, *J* = 6.6 Hz, 2H), 3.04 – 2.96 (m, 2H), 2.51 (s, 6H), 2.42 (s, 6H), 2.33 (t, *J* = 7.0 Hz, 2H), 2.00 – 1.90 (m, 2H), 1.57 – 1.46 (m, 4H), 1.44 (s, 9H), 1.39 – 1.30 (m, 2H). ^{13}C NMR (101 MHz, $CDCl_3$) δ 156.30, 154.13, 152.80, 145.52, 140.67, 131.59, 121.86, 40.27, 39.57, 36.41, 29.93, 29.18, 28.54, 27.69, 27.58, 23.44, 16.55, 14.60.

N-(5-Aminopentyl)-4-BODIPY-butanamide (**17a**)

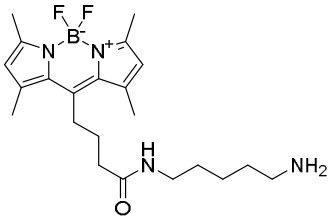

To a solution of **17** (206 mg, 0.40 mmol) in DCM (15 mL), TFA (1.0 mL, 13 mmol) was added under inert atmosphere and the reaction mixture was stirred for 16 hours at RT. The resulting mixture was concentrated to yield the title compound as a dark red solid. LC/MS showed partial removal of BF_2-group by TFA. The impure product (68 mg) was used without further purification for subsequent reactions. ^{1}H NMR (400 MHz, MeOD) δ 6.15 (d, *J* = 8.1 Hz, 2H), 3.19 (t, *J* = 7.1 Hz, 2H), 3.09 – 2.97 (m, 2H), 2.71 (t, 2H), 2.45 (d, *J* = 4.9 Hz, 12H), 2.41 – 2.34 (m, 2H), 2.01 – 1.87 (m, 2H), 1.61 – 1.44 (m, 4H), 1.44 – 1.33 (m, 2H).

10-(Ethoxyfluorophosphoryl)decyl (5-(4-BODIPY-butanamido)pentyl)carbamate (**3**, BODIPY-FP)

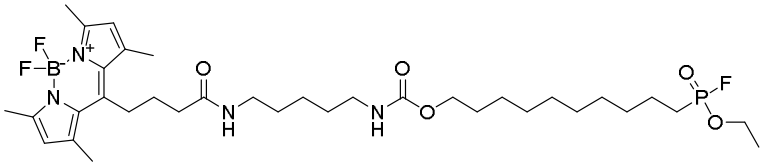

17a (68 mg) was placed under inert atmosphere and dissolved in DCM (3 mL). Dry DMF (2 mL) was added and **14** (42 mg, 0.10 mmol) was added to the solution. The reaction mixture was stirred for 4 hours at RT. The reaction was quenched with water (5 mL) and EtOAc (5 mL) was added. The aqueous layer was extracted with EtOAc (2x) and DCM (2x). The combined organic layers were dried ($MgSO_4$), filtered and concentrated. Purification was performed using silica column chromatography (100% EtOAc) to yield 39 mg of crude product. Further purification was performed on preparative HPLC (H_2O/acetonitrile/TFA). Pure fractions were combined and lyophilized to obtain the title compound as a red solid (19 mg, 27 µmol, 26%). ^{1}H NMR (500 MHz, $CDCl_3$) δ 6.05 (s, 2H), 5.79 (s, 1H), 4.72 (s, 1H), 4.33 – 4.19 (m, 2H), 4.07 – 3.96 (m, 2H), 3.29 – 3.20 (m, 2H), 3.20 – 3.11 (m, 2H), 3.05 – 2.95 (m, 2H), 2.51 (s, 6H), 2.43 (s, 6H), 2.39 – 2.29 (m, 2H), 2.01 – 1.93 (m, 2H), 1.93 – 1.83 (m, 2H), 1.71 – 1.47 (m, 8H), 1.43 – 1.24 (m, 17H). ^{13}C NMR (126 MHz, $CDCl_3$) δ 171.77, 157.02, 154.04, 145.32, 140.49, 131.48, 121.74, 64.96, 63.09 (d, *J* = 7.2 Hz), 40.45, 39.47, 36.27, 30.23 (d, *J* = 16.8 Hz), 29.71, 29.37, 29.16, 29.13, 29.01, 28.92 – 28.77 (m), 27.56, 27.49, 25.82, 24.94 – 23.29 (m), 21.85 (d, *J* = 5.2 Hz), 16.45, 16.35 (d, *J* = 5.6 Hz), 14.47. ^{19}F NMR (471 MHz, $CDCl_3$) δ -64.70 (d, *J* = 1070 Hz), -144.63 – -150.06 (m). ^{31}P NMR (202 MHz, $CDCl_3$) δ 31.96 (d, *J* = 1070 Hz). HRMS: $[M+H]^+$ calculated for $C_{35}H_{58}BF_3N_4O_5P$: 713.4184; found: 713.4194

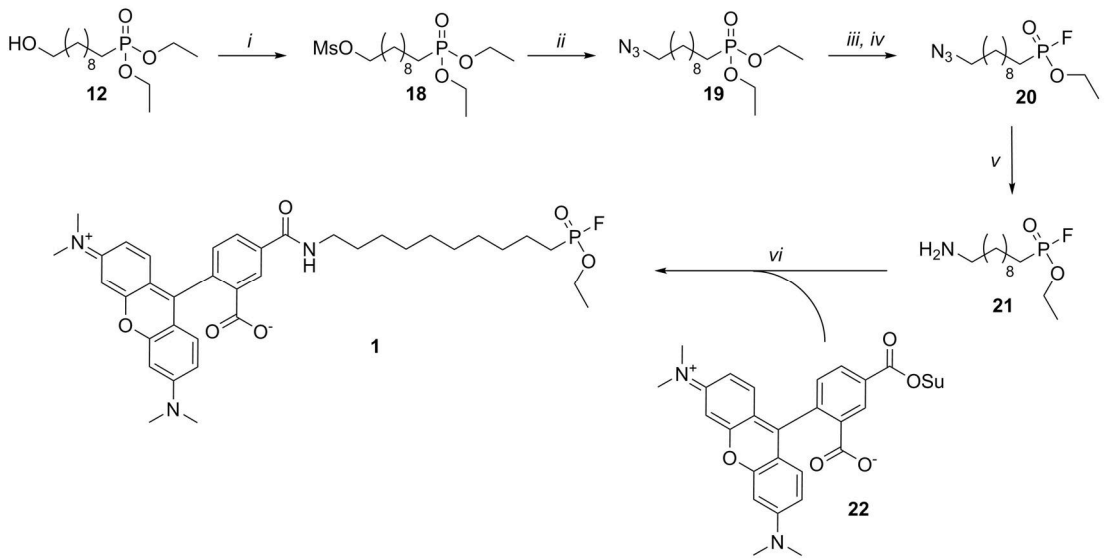

Scheme S6.2 | Synthesis of commercially available TAMRA-FP probe **1.** Reagents and conditions: *i*) MsCl, DIPEA, DCM, 0-20 °C; *ii*) NaN_3, DCM, DMF, 50 °C, 45%; *iii*) oxalyl chloride, DCM, 0-20 °C; *iv*) DAST, DCM, -78 °C, 83%; *v*) trimethylphospine, THF, 0-20 °C; *vi*) 5-TAMRA SE (**22**), NEt_3, DCM, RT, 54%.

10-(Diethoxyphosphoryl)decyl methanesulfonate (**18**)

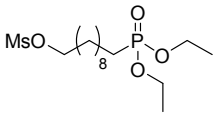

Diethyl (10-hydroxydecyl)phosphonate **12** (147 mg, 0.50 mmol) was dissolved in dry DCM (10 mL) and cooled to 0 °C. Methanesulfonyl chloride (43 µL, 63 mg, 0.55 mmol) and DIPEA (96 µL, 71 mg, 0.55 mmol) were added and the mixture is left to stir for 20 hours, warming to RT. The reaction was quenched by the addition of aqueous HCl (2 N) solution. The aqueous layer was extracted three times with DCM. The combined organic layers were dried ($MgSO_4$), filtered and concentrated yielding crude mesylated product which was used directly in the next reaction.

Diethyl (10-azidodecyl)phosphonate (**19**)

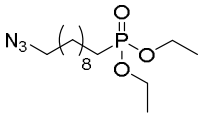

10-(diethoxyphosphoryl)decyl methanesulfonate **18** (186 mg, 0.50 mmol) was dissolved in dry DCM (5 mL). Dry DMF (5 mL) and sodium azide (98 mg, 1.50 mmol) were added and the mixture was stirred at 50 °C for 72 h. The crude mixture was poured into saturated aqueous $NaHCO_3$ and after separation of the layers the water layer was

extracted twice with DCM. The combined organic layers were dried ($MgSO_4$), filtered, and concentrated. Purification by column chromatography (50-90% EtOAc in pentane) afforded the product as a colourless oil (71 mg, 0.22 mmol, 45% yield over two steps). ^{1}H NMR (400 MHz, $CDCl_3$) δ 4.19 – 4.01 (m, 4H), 3.26 (t, *J* = 7.0 Hz, 2H), 1.80 – 1.66 (m, 2H), 1.66 – 1.52 (m, 4H), 1.42 – 1.20 (m, 18H). ^{13}C NMR (101 MHz, $CDCl_3$) δ 61.43 (d, *J* = 6.5 Hz), 51.48, 30.69, 30.52, 29.42, 29.27, 29.13, 29.07, 28.85, 26.72, 25.67 (d, *J* = 140.3 Hz), 22.41 (d, *J* = 5.2 Hz), 16.51 (d, *J* = 6.0 Hz).

Ethyl (10-azidodecyl)phosphonofluoridate (**20**)

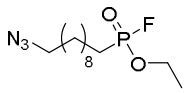

19 (71 mg, 0.22 mmol) was dissolved in dry DCM (5 mL) and stirred on ice. Oxalyl chloride (1.11 mL, 2.22 mmol) was added and stirred overnight, warming up to RT. The reaction was quenched by the addition of water (5 mL), diluted with DCM (5 mL) and stirred for 10 minutes. A cloudy suspension formed. The water layer was separated and extracted twice with DCM (water layer still cloudy) and twice with EtOAc (water layer now clear). The organic layers were combined, dried ($MgSO_4$), filtered and concentrated. The crude ethyl (10-azidodecyl)phosphonate was brought under nitrogen atmosphere, dissolved in dry DCM (3 mL) and cooled to -78 °C. Diethylamino sulfurtrifluoride (88 µL, 0.67 mmol) was added and the resulting mixture stirred at -78 °C for 30 minutes. The reaction was quenched by the addition of a 1:1 mixture (v/v) of water:EtOAc (10 mL). The water layer was separated and extracted twice with EtOAc. The organic layers were combined, dried ($MgSO_4$), filtered, and concentrated. Purification by column chromatography (50-100 % EtOAc in pentane) yielded the title compound (54 mg, 0.18 mmol, 83%). ^{1}H NMR (500 MHz, $CDCl_3$) δ 4.32 – 4.21 (m, 2H), 3.26 (t, *J* = 7.0 Hz, 2H), 1.95 – 1.83 (m, 2H), 1.72 – 1.54 (m, 4H), 1.46 – 1.15 (m, 15H). ^{13}C NMR (126 MHz, $CDCl_3$) δ 63.11 (d, *J* = 7.2 Hz), 51.55, 30.40, 30.27, 29.43, 29.24, 29.16, 29.00, 28.91, 26.76, 24.38 (dd, *J* = 22.3, 143.1 Hz), 21.97 (d, *J* = 5.5 Hz), 16.43 (d, *J* = 5.6 Hz).^{31}P NMR (202 MHz, $CDCl_3$) δ 32.44 (d, *J* = 1070 Hz). ^{19}F NMR (471 MHz, $CDCl_3$) δ -64.99 (d, *J* = 1070 Hz).

Ethyl (10-aminodecyl)phosphonofluoridate (**21**)

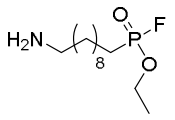

Ethyl (10-azidodecyl)phosphonofluoridate **20** (18 mg, 0.061 mmol) was coevaporated with dry toluene, dissolved in dry THF (5 mL) and cooled on ice. Trimethylphosphine (0.123 mL, 0.123 mmol) was added as a solution in THF (1 M). The resulting mixture was stirred for 3 h at 0°C after which water (0.2 mL) was added. The crude was concentrated *in vacuo* and coevaporated twice with dry toluene. The resulting crude product was used without further purification for the next reaction.

2-(3,6-Bis(dimethylamino)xanthylium-9-yl)-5-((10-(ethoxyfluorophosphoryl)decyl)carbamoyl)benzoate (**1**, FP-TAMRA)

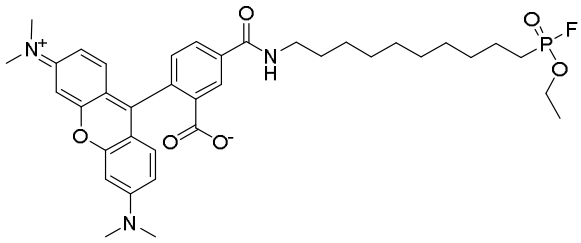

Crude **21** was dissolved in dry DCM and 5-TAMRA succinimidyl ester **22** (5.0 mg, 9.5 µmol) and triethylamine (7.9 µL, 0.057 mmol) were added. The mixture was stirred at RT overnight. TLC showed complete conversion (10% MeOH/EtOAc). The reaction mixture was concentrated *in vacuo* and purified by preparative HPLC. After lyophilization a purple powder was obtained of sufficient (>90 %) purity (3.47 mg, 5.10 µmol, 54% yield over two steps). HRMS: $[M+H]^+$ calculated for $C_{37}H_{48}FN_3O_6P$: 680.3259; found: 680.3250.

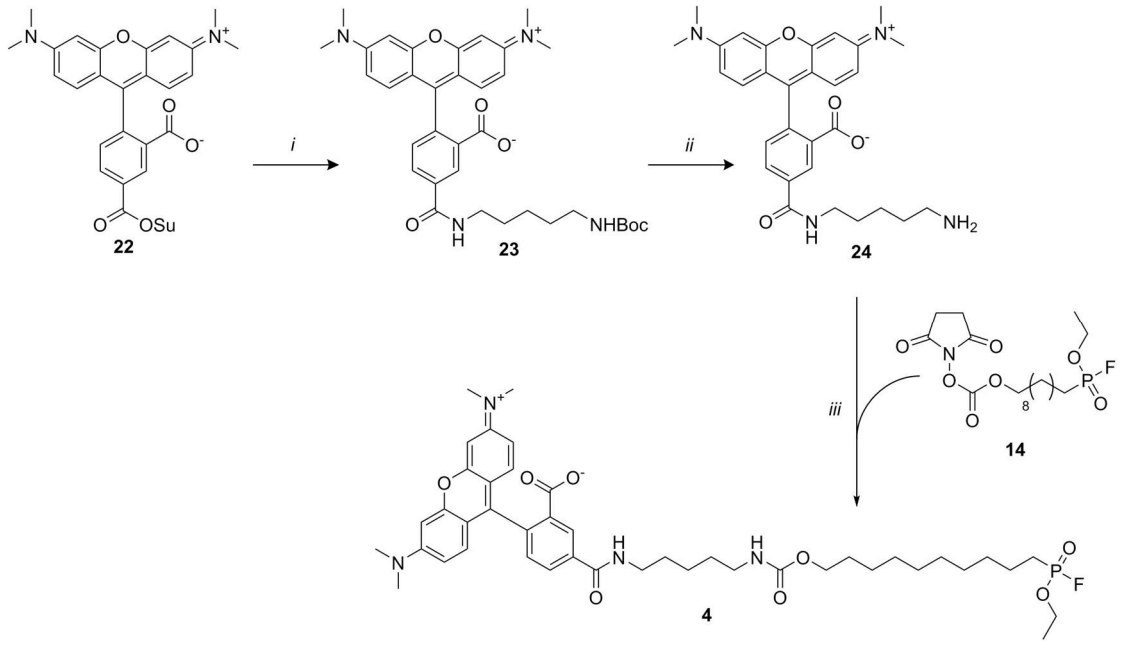

Scheme S6.3 | Synthesis of probe **4**. Reagents and conditions: *i*) *N*-Boc cadaverine, DCM, DMF, RT; *ii*) TFA, DCM, RT; *iii*) **14**, NEt_3, DCM, DMF, RT, 70%.

tert-Butyl (5-(5-TAMRA-amino)pentyl)carbamate (**23**)

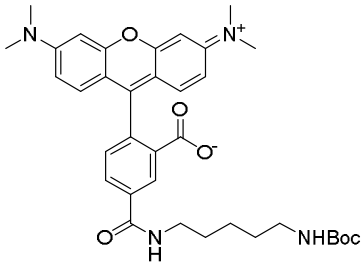

5-TAMRA-succinimidyl ester **22** (5.0 mg, 9.5 µmol) was dissolved in DCM (1.5 mL) and DMF (1 mL). To this solution *N*-Boc cadaverine (2.6 µL, 12 µmol) and TEA (2.4 µL, 17 µmol) were added. The reaction mixture was stirred for 4 hours at room temperature. LC/MS showed full conversion of **22**. The solvents were removed under low pressure to afford the crude product as a pink solid. The resulting crude product was used in subsequent reactions without further purification.

5-(5-TAMRA-amino)pentan-1-amine (**24**)

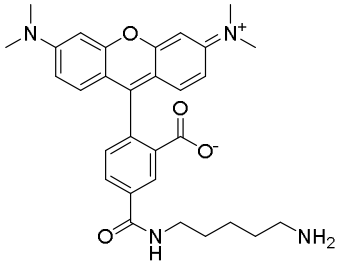

23 was dissolved in DCM (1.4 mL) and TFA (0.1 mL). The reaction mixture was stirred for 3 hours at room temperature, after which LC/MS showed full conversion of **23**. The solvent was removed under low pressure to afford the crude product as a red solid. The resulting crude product was used in subsequent reactions without further purification.

10-(Ethoxyfluorophosphoryl)decyl (5-(4-(3,6-bis(dimethylamino)xanthylium-9-yl)-3-carboxybenzamido)) pentylcarbamate (**4**)

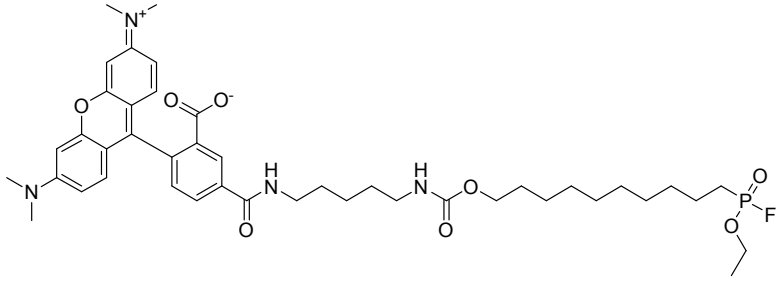

24 was dissolved in DCM (1.5 mL) and DMF (1 mL) and placed under inert atmosphere. **14** (19 mg, 46 µmol) and TEA (7.0 µL, 50 µmol) were added to the solution. The reaction mixture was stirred for 4 hours at room temperature. The solvent was removed under low pressure and purification was performed with preparative HPLC (50-55% acetonitrile in water, 0.1% TFA). Pure fractions were combined, extracted to 1,4-dioxane and lyophilized to yield the title compound as a purple solid (5.4 mg,

5.8 µmol, 61% over three steps). ^{1}H NMR (500 MHz, $CDCl_3$) δ 8.75 (s, 1H), 8.29 (d, *J* = 7.8 Hz, 1H), 8.17 (s, 1H), 7.30 (d, *J* = 7.8 Hz, 1H), 7.19 (d, *J* = 9.4 Hz, 2H), 6.86 (dd, *J* = 9.5, 2.4 Hz, 2H), 6.74 (d, *J* = 2.4 Hz, 2H), 4.98 (s, 1H), 4.30 – 4.20 (m, 2H), 4.13 – 3.96 (m, 2H), 3.50 (q, *J* = 6.7 Hz, 2H), 3.28 (s, 12H), 3.16 (d, *J* = 16.4 Hz, 2H), 1.96 – 1.80 (m, 2H), 1.78 – 1.51 (m, 8H), 1.50 – 1.22 (m, 17H). ^{31}P NMR (202 MHz, $CDCl_3$) δ 32.15 (d, *J* = 1070 Hz). ^{19}F NMR (471 MHz, $CDCl_3$) δ -64.99 (d, *J* = 1070 Hz). HRMS: $[M+H]^+$ calculated for $C_{43}H_{59}FN_4O_8P$: 809.4049; found: 809.4059.

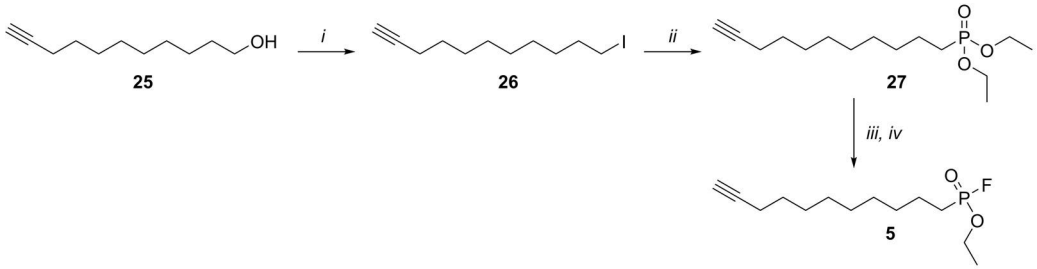

Scheme S6.4 | Synthesis of 'dark' alkyne-FP (**5**). Reagents and conditions: *i*) PPh_3, imidazole, I_2, DCM, RT, 20%; *ii*) $P(OEt)_3$, 160 °C, quantitative; *iii*) oxalyl chloride, DCM; *iv*) DAST, DCM, -78 °C, 41%.

11-Iodoundec-1-yne (**26**)

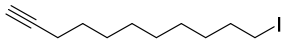

Imidazole (102 mg, 1.4 mmol) and triphenylphosphine (355 mg, 1.35 mmol) were dissolved in DCM (10 mL) and iodine (330 mg, 1.3 mmol) was added gradually. After stirring for 20 min at RT, a solution of **25** (172 mg, 1.0 mmol) in DCM (5 mL) was added dropwise to the reaction mixture. After stirring for 16 h a solution of additional imidazole (102 mg, 1.5 mmol), PPh_3 (393 mg, 1.5 mmol) and I_2 (381 mg, 1.5 mmol) in THF (15 mL) was added to the reaction mixture. After 2 h an aqueous solution of $Na_2S_2O_3$ (10 mL, 1 M) was added to quench the reaction. The layers were separated and the organic layer was dried ($MgSO_4$), filtered and concentrated *in vacuo*. Purification by column chromatography (0-5% EtOAc in pentane) yielded the title compound as a yellow oil (58 mg, 0.20 mmol, 20%). ^{1}H NMR (400 MHz, $CDCl_3$) δ 3.19 (t, *J* = 7.0 Hz, 2H), 2.18 (td, *J* = 2.6, 7.1 Hz, 2H), 1.94 (t, *J* = 2.6 Hz, 1H), 1.90 – 1.76 (m, 2H), 1.58 – 1.47 (m, 2H), 1.40 – 1.33 (m, 4H), 1.33 – 1.19 (m, 6H). ^{13}C NMR (101 MHz, $CDCl_3$) δ 84.73, 68.13, 33.54, 30.49, 30.33, 29.28, 29.01, 28.69, 28.49, 18.41, 7.35.

Diethyl undec-10-yn-1-ylphosphonate (**27**)

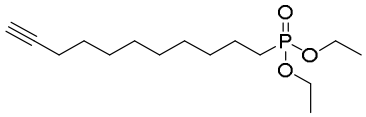

Compound **28** (58 mg, 0.20 mmol) was dissolved in triethyl phosphite (500 µL) and heated to reflux. After stirring for 4 h the reaction mixture was cooled to RT and concentrated *in vacuo* at 75 °C yielding compound **27** (60 mg, 0.20 mmol, quantitative yield) as a yellow oil that was used without further purification. ^{1}H NMR (400 MHz, $CDCl_3$) δ 4.20 – 4.02 (m, 4H), 2.18 (td, *J* = 7.0, 2.7 Hz, 2H), 1.95 (t, *J* = 2.7 Hz, 1H), 1.81 – 1.66 (m, 2H), 1.65 – 1.56 (m, 2H), 1.56 – 1.47 (m, 2H), 1.46 – 1.22 (m, 16H). ^{13}C NMR (101 MHz, $CDCl_3$) δ 84.77, 68.17, 61.65 – 61.32 (m), 30.72, 30.55, 30.37, 29.77, 29.27, 29.08, 28.74, 28.50, 25.72 (d, *J* = 140.4 Hz), 22.44 (d, *J* = 5.2 Hz), 18.44, 16.55 (d, *J* = 6.1 Hz).

Ethyl undec-10-yn-1-ylphosphonofluoridate (**5**)

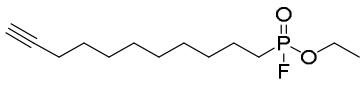

A solution of oxalyl chloride in DCM (2.0 M, 1.0 mL, 2.0 mmol) was added to **27** (60 mg, 0.20 mmol) and the reaction mixture was stirred overnight at RT. DCM and H_2O were added and after 10 min of stirring the layers were separated and the aqueous layer was extracted two times with DCM. The combined organic layers were dried ($MgSO_4$), filtered and concentrated *in vacuo*. The crude product was coevaporated twice with toluene and redissolved in DCM. The reaction mixture was cooled to -78 °C, after which DAST (110 µL, 0.83 mmol) was added. After stirring for 30 min the reaction mixture was quenched with H_2O and aqueous layer was extracted three times with DCM. The combined organic layers were dried ($MgSO_4$), filtered and concentrated *in vacuo*. Purification by column chromatography yielded the title compound (17 mg, 64 µmol, 32%) as a yellow oil. ^{1}H NMR (400 MHz, $CDCl_3$) δ 4.32 – 4.20 (m, 2H), 2.18 (td, *J* = 2.6, 7.1 Hz, 2H), 1.94 (t, *J* = 2.7 Hz, 1H), 1.93 – 1.82 (m, 2H), 1.73 – 1.58 (m, 2H), 1.58 – 1.47 (m, 2H), 1.44 – 1.26 (m, 13H). ^{13}C NMR (101 MHz, $CDCl_3$) δ 84.85, 68.24, 63.16 (d, *J* = 7.3 Hz), 30.48, 30.31, 29.26, 29.11, 29.03, 28.79, 28.56, 24.43 (dd, *J* = 22.3, 143.0 Hz), 22.02 (d, *J* = 5.6 Hz), 18.51, 16.50 (d, *J* = 5.8 Hz). ^{31}P NMR (162 MHz, $CDCl_3$) δ 32.37 (d, *J* = 1070 Hz). ^{19}F NMR (471 MHz, $CDCl_3$) δ -64.98 (d, *J* = 1070 Hz). HRMS: $[M+Na]^+$ calculated for $C_{13}H_{24}FNaO_2P$: 285.1390; found: 285.1395.

Supplementary Tables and Figures

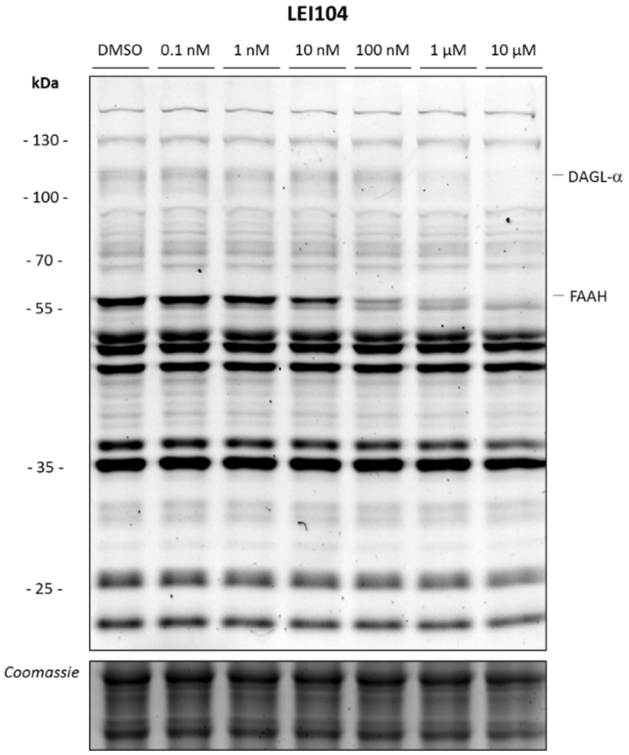

Figure S6.1 | Identification of DAGL-α labeling by probe **3** (500 nM) in mouse brain membrane proteome. LEI104 shows identical inhibition profile of the band at 120 kDa as reported previously when labeled with MB064 (**2**).[9]

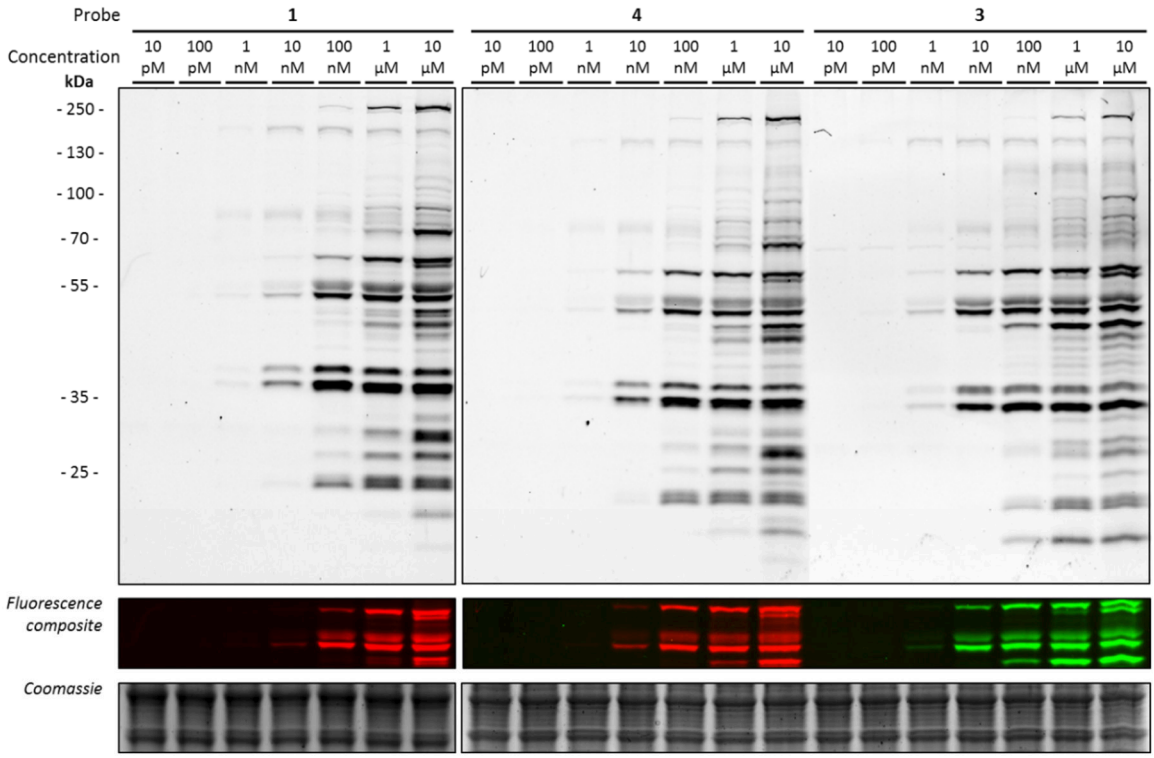

Figure S6.2 | Representative gels of the dose response analysis of the three probes of Figure 6.3. Final quantification was based on 3 gels.

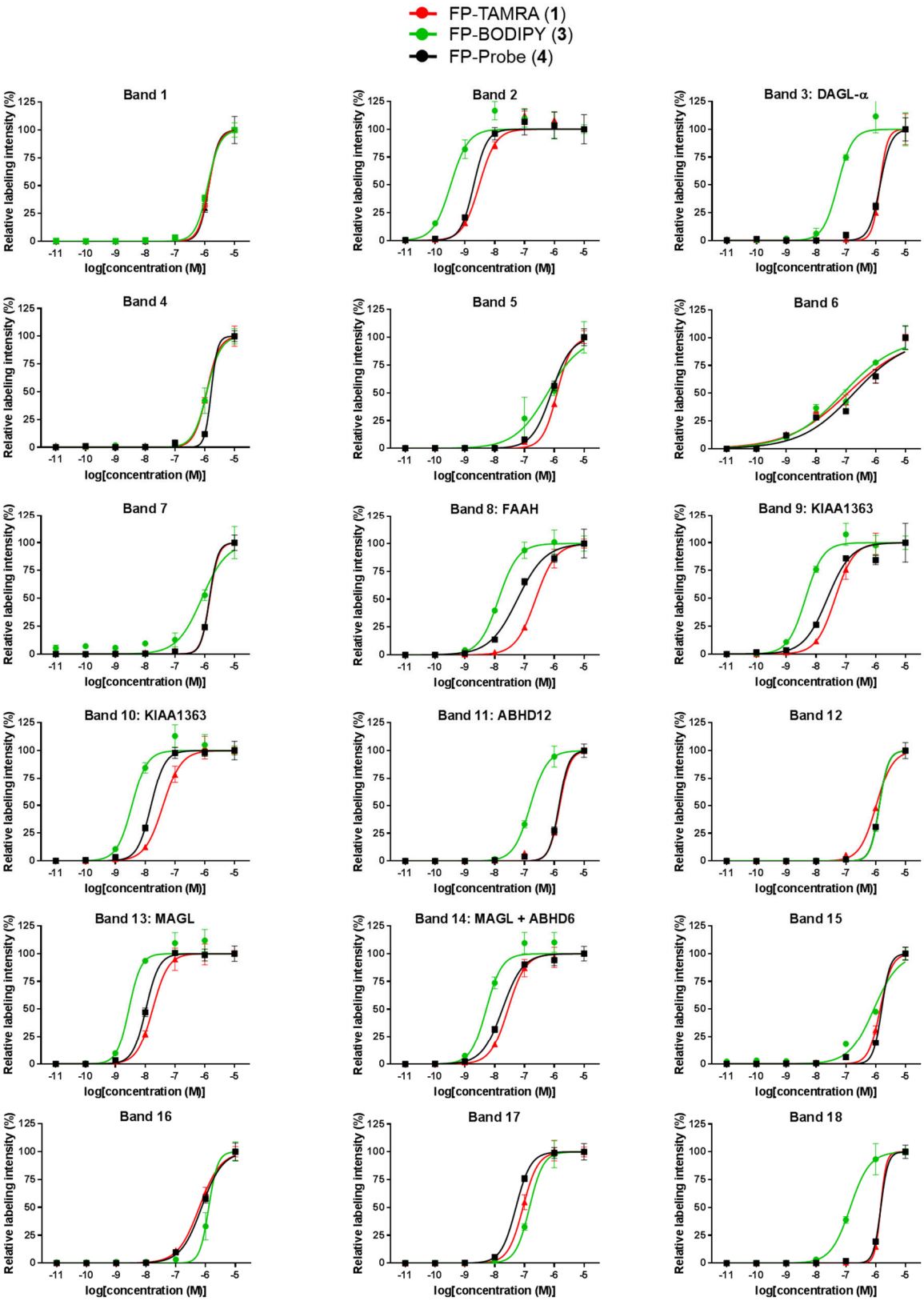

Figure S6.3 | EC_{50} curves of the 18 quantified bands of Figure 6.3.

Table S6.1 | Overview of pEC_{50} values of FP probes **1**, **3** and **4**. Band numbers correspond to Figure 6.3.

	Probe 1		Probe 3		Probe 4	
Band	pEC_{50}	± SEM	pEC_{50}	± SEM	pEC_{50}	± SEM
1	≤ 6	-	≤ 6	-	≤ 6	-
2	8.52	0.07	9.48	0.12	8.71	0.17
3	≤ 6	-	7.28	0.09	≤ 6	-
4	≤ 6	0.04	≤ 6	-	≤ 6	-
5	≤ 6	-	≤ 6	-	≤ 6	-
6	6.94	0.13	7.10	0.15	6.73	0.14
7	≤ 6	-	≤ 6	-	≤ 6	-
8	6.63	0.05	7.87	0.07	7.24	0.08
9	7.36	0.07	8.35	0.08	7.62	0.11
10	7.4	0.07	8.45	0.10	7.80	0.07
11	≤ 6	-	6.80	0.05	≤ 6	-
12	≤ 6	-	5.87	0.09	≤ 6	-
13	7.75	0.07	8.55	0.13	7.98	0.03
14	7.55	0.07	8.28	0.09	7.74	0.05
15	≤ 6	-	6.22	0.09	≤ 6	-
16	6.21	0.04	≤ 6	-	6.09	0.04
17	7.05	0.04	6.83	0.06	7.29	0.05
18	≤ 6	-	6.85	0.05	≤ 6	-

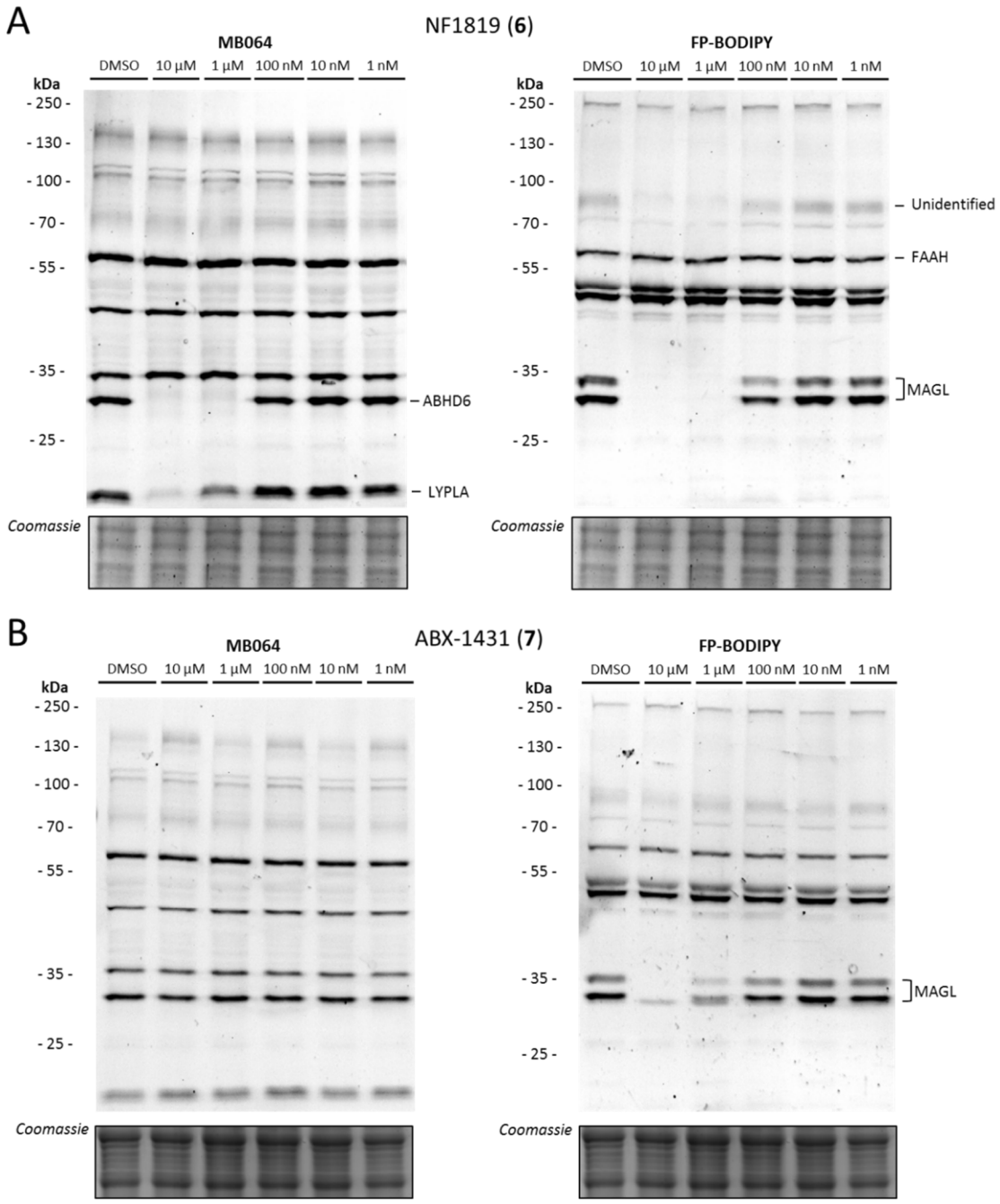

Figure S6.4 | Dose response inhibition of the probe cocktail by NF1819 (**6**) (A) and ABX-1431 (**7**) (B) in mouse brain membrane proteome, split by fluorescence channel to visualize overlapping bands of MAGL and ABHD6.

References

1. Long, J. Z. & Cravatt, B. F. The Metabolic Serine Hydrolases and Their Functions in Mammalian Physiology and Disease. *Chem. Rev.* **111**, 6022–6063 (2011).
2. Shahiduzzaman, M. & Coombs, K. M. Activity based protein profiling to detect serine hydrolase alterations in virus infected cells. *Front. Microbiol.* **3**, 1–5 (2012).
3. Wang, S. *et al.* Advanced Activity-Based Protein Profiling Application Strategies for Drug Development. *Front. Pharmacol.* **9**, (2018).
4. Simon, G. M. & Cravatt, B. F. Activity-based Proteomics of Enzyme Superfamilies: Serine Hydrolases as a Case Study. *J. Biol. Chem.* **285**, 11051–11055 (2010).
5. Liu, Y., Patricelli, M. P. & Cravatt, B. F. Activity-based protein profiling: The serine hydrolases. *Proc. Natl. Acad. Sci.* **96**, 14694–14699 (1999).
6. van Esbroeck, A. C. M. *et al.* Activity-based protein profiling reveals off-target proteins of the FAAH inhibitor BIA 10-2474. *Science* **356**, 1084–1087 (2017).
7. van Rooden, E. J. *et al.* Mapping in vivo target interaction profiles of covalent inhibitors using chemical proteomics with label-free quantification. *Nat. Protoc.* **13**, 752–767 (2018).
8. Hoover, H. S., Blankman, J. L., Niessen, S. & Cravatt, B. F. Selectivity of inhibitors of endocannabinoid biosynthesis evaluated by activity-based protein profiling. *Bioorg. Med. Chem. Lett.* **18**, 5838–41 (2008).
9. Baggelaar, M. P. *et al.* Development of an Activity-Based Probe and In Silico Design Reveal Highly Selective Inhibitors for Diacylglycerol Lipase-α in Brain. *Angew. Chemie Int. Ed.* **52**, 12081–12085 (2013).
10. Adam, G. C., Sorensen, E. J. & Cravatt, B. F. Proteomic profiling of mechanistically distinct enzyme classes using a common chemotype. *Nat. Biotechnol.* **20**, 805–809 (2002).
11. de Bruin, G. *et al.* A Set of Activity-Based Probes to Visualize Human (Immuno)proteasome Activities. *Angew. Chemie Int. Ed.* **55**, 4199–4203 (2016).
12. Patricelli, M. P., Giang, D. K., Stamp, L. M. & Burbaum, J. J. Direct visualization of serine hydrolase activities in complex proteomes using fluorescent active site-directed probes. *Proteomics* **1**, 1067–1071 (2001).
13. Tully, S. E. & Cravatt, B. F. Activity-Based Probes That Target Functional Subclasses of Phospholipases in Proteomes. *J. Am. Chem. Soc.* **132**, 3264–3265 (2010).
14. Johnson, D. S. *et al.* Discovery of PF-04457845: A Highly Potent, Orally Bioavailable, and Selective Urea FAAH Inhibitor. *ACS Med. Chem. Lett.* **2**, 91–96 (2011).
15. Ogasawara, D. *et al.* Rapid and profound rewiring of brain lipid signaling networks by acute diacylglycerol lipase inhibition. *Proc. Natl. Acad. Sci.* **113**, 26–33 (2016).
16. Baggelaar, M. P. *et al.* Highly Selective, Reversible Inhibitor Identified by Comparative Chemoproteomics Modulates Diacylglycerol Lipase Activity in Neurons. *J. Am. Chem. Soc.* **137**, 8851–8857 (2015).
17. Ogura, Y., Parsons, W. H., Kamat, S. S. & Cravatt, B. F. A calcium-dependent acyltransferase that produces N-acyl phosphatidylethanolamines. *Nat. Chem. Biol.* **12**, 669–671 (2016).
18. Pan, B. *et al.* Blockade of 2-arachidonoylglycerol hydrolysis by selective monoacylglycerol lipase inhibitor 4-nitrophenyl 4-(dibenzo[d][1,3]dioxol-5-yl(hydroxy)methyl)piperidine-1-carboxylate (JZL184) Enhances retrograde endocannabinoid signaling. *J. Pharmacol. Exp. Ther.* **331**, 591–7 (2009).
19. Bisogno, T. *et al.* Cloning of the first sn1-DAG lipases points to the spatial and temporal regulation of endocannabinoid signaling in the brain. *J. Cell Biol.* **163**, 463–468 (2003).
20. Brindisi, M. *et al.* Development and Pharmacological Characterization of Selective Blockers of 2-Arachidonoyl Glycerol Degradation with Efficacy in Rodent Models of Multiple Sclerosis and Pain. *J. Med. Chem.* **59**, 2612–2632 (2016).
21. Lim, J. *et al.* Endocannabinoid Modulation of Predator Stress-Induced Long-Term Anxiety in Rats. *Neuropsychopharmacology* **41**, 1329–1339 (2015).
22. Blankman, J. L. *et al.* Methods of treating inflammation or neuropathic pain (WO2016183097A1). (2015).
23. Justin S. Cisar *et al.* Carbamate compounds and of making and using same (US20150018335A1). (2012).
24. Cisar, J. S. *et al.* Identification of ABX-1431, a Selective Inhibitor of Monoacylglycerol Lipase and Clinical Candidate for Treatment of Neurological Disorders. *J. Med. Chem.* **61**, 9062–9084 (2018).